Reduced High-Latitude Land Seasonality in Climates with Very High Carbon Dioxide

Matthew Henry* and Geoffrey K. Vallis

Department of Mathematics, University of Exeter, Exeter, UK

**Corresponding author*: Matthew Henry, m.henry@exeter.ac.uk, @mattjohenry

ABSTRACT

Observations of warm past climates and projections of future climate change show that the Arctic warms more than the global mean, particularly during winter months. Past warm climates such as the early Eocene had above-freezing Arctic continental temperatures year-round. In this paper, we show that a reduced Arctic land seasonality with increased greenhouse gases is a robust consequence of the smaller surface heat capacity of land (compared to ocean), without recourse to other processes or feedbacks. We use a General Circulation Model (GCM) with no clouds or sea ice and a simple representation of land. The equator-to-pole surface temperature gradient falls with increasing CO_2, but this is only a near-surface phenomenon and occurs with little change in total meridional heat transport. The high-latitude land has about twice as much warming in winter than in summer, whereas high-latitude ocean has very little seasonality in warming. A surface energy balance model shows how the combination of the smaller surface heat capacity of land and the nonlinearity of the temperature dependence of surface longwave emission gives rise to the seasonality of land surface temperature change. The atmospheric temperature change is surface-enhanced in winter as the atmosphere is near radiative-advective equilibrium, but more vertically homogeneous in summer as the Arctic land gets warm enough to trigger convection. While changes in clouds, sea ice, and ocean heat transport undoubtedly play a role in high latitude warming, these results show that enhanced land surface temperature change and surface-enhanced atmospheric temperature change in winter can happen in their absence for very basic and robust reasons.

Plain language significance statement

As we add greenhouse gases to the atmosphere, the Earth's surface gets warmer and this is especially pronounced in the Arctic in winter. For the current and near-future climate, this is at least in part due to the melting of sea ice. However, as time progresses all the sea ice melts, and even after that climate models show enhanced polar warming, with most of the warming occurring over Arctic land in winter. Moreover, fossils indicate that the very warm climates of the past (some 50 million years ago for example) had exceptionally warm Arctic winters. Previous work has attributed this reduced seasonality over Arctic land to the effects of sea ice or clouds. Here, we identify a robust mechanism, based on the smaller heat capacity of land and the fact that cold bodies need to warm more to reach a given increase in radiation, as to why Arctic land should have a reduced seasonality in very warm climates. The mechanism depends neither on sea ice nor clouds.

1. Introduction

The early Eocene (48–56 million years ago) had an 'equable climate', with a smaller equator-to-pole temperature gradient than today, at least at the surface, with year-round above-freezing temperatures at high latitude continents. Proxy records indicate that at latitudes around 75 degrees North, the annual-mean temperature was about 8°C, the cold month mean temperature was between 0°C and 3.5°C, and the warm month mean temperature was between 19°C and 20°C (Eberle et al. 2010; Evans et al. 2018). Carbon dioxide concentrations in the early Eocene are uncertain, and have been variously estimated to be as little as 600 ppm or well over 4000 ppm (Beerling and Royer 2011).

Understanding the temperature structure under such conditions is sometimes called the 'equable climate problem', since although very warm high latitudes can be achieved simply with very high values of CO_2 or other greenhouse gases, simulations often give rise to very high tropical temperatures, possibly incompatible with proxy records (Huber and Caballero 2011). However, the incompatibility is itself uncertain as more recent proxies of early Eocene tropical SSTs do indicate temperatures warmer than previously estimated, and tropical temperature estimates tend to have large error margins (Pearson et al. 2007). Nevertheless, the balance of evidence is that in equable climates, the increase in temperature at high latitudes (over the temperature of today) was greater than the increase at low latitudes, at least in winter months. This result is not fully understood, for it implies either a greater meridional heat transport in the atmosphere-ocean system or a change in the vertical temperature structure of the atmosphere, or some change in seasonality, or a combination of these effects. Maintaining above-freezing temperatures over land in high-latitude winter seems particularly problematic, since the low heat capacity of land suggests that temperatures will cool rapidly in winter when there is no incoming solar radiation.

As in past warm climates, the surface temperature change at high latitudes is amplified in projections of future climate change (Holland and Bitz 2003). This has been variously attributed to the surface albedo feedback (critically discussed by Winton 2006), a temperature feedback (Pithan and Mauritsen 2014), and increased meridional atmospheric energy transport (Hwang and Frierson 2010). Investigation of the vertical structure of temperature change also shows that, at high latitudes, the CO_2 forcing and water vapor feedback lead to surface enhanced warming (Taylor et al. 2013; Henry et al. 2020), in contrast to the tropics where convection fixes the vertical structure of temperature to the moist adiabat. The surface albedo feedback also increases high latitude surface warming but leads to a decrease in the dry component of atmospheric energy transport convergence (Hwang et al. 2011; Henry et al. 2020).

A number of simulations with comprehensive General Circulation Models (GCMs) have addressed these issues, both for past climates and future warming. Thus, for example, Huber and Caballero (2011) show that, by increasing CO_2 to high but feasible concentrations in a fully-coupled general circulation model (GCM), sufficient winter polar amplification occurs over land to maintain above-freezing temperatures. The possible range of appropriate levels of CO_2 concentration to best represent the early Eocene is still rather wide though — they suggest between 2500 ppm and 6500 ppm. Other models have given different results and the mechanisms responsible for enhanced winter warming are still debated. For example, Abbot and Tziperman (2008) show that deep convection and consequent cloud longwave radiative forcing can maintain warm Arctic temperatures over winter in high CO_2 climates and Cronin and Tziperman (2015) discuss the role of low clouds in the formation of Arctic continental air masses. In winter, maritime air masses are advected onto continents: if their initial state is warmer, they are more likely to form low clouds which suppresses surface radiative cooling and amplifies the continental surface warming. They report a two degrees increase in continental surface temperatures for every degree of initial maritime near surface air temperature increase. Furthermore, Lunt et al. (2012) find that differences between GCM simulations of the early Eocene are mainly due to clear-sky longwave feedbacks, surface albedo feedbacks, and aerosol loading, rather than cloud feedbacks or boundary conditions.

The amplified Arctic winter warming under anthropogenic global warming has been attributed to increased seasonal heat storage in the ocean in summer from the surface albedo feedback and consequent increased ocean heat release in winter which, in combination with a surface-enhanced vertical structure of atmospheric temperature change, potentially leads to more warming in winter (Bintanja and Van der Linden 2013; Pithan and Mauritsen 2014). A rather different explanation is given by Lu and Cai (2009), who analyze the surface energy budget of comprehensive climate models. They find that the increased winter warming is due to the clear-sky longwave feedback, including the effects of a lapse rate change. Evidently, the roles of sea ice, seasonal heat storage, and the lapse rate change on the seasonality of polar amplification remain unclear, in part due to the difficulties of analyzing comprehensive climate models.

Our goal in this paper is to isolate and thereby better understand the various mechanisms involved in high latitude warming. The detailed configurations differ considerably between past warm climates and future anthropogenic warming (e.g. the presence of sea ice and the differing continental configurations), hence we focus on robust effects that can apply in both situations. To this end, we use a GCM with no sea ice, clouds or ocean circulation, but with land-ocean contrasts and a comprehensive radiation scheme (Manners et al. 2017). We find that high latitude land warms more in winter and less in summer compared to the high latitude ocean, in response to an increase in CO_2 concentration. Moreover, the high latitude atmospheric temperature change is surface-enhanced in winter and more vertically homogeneous in summer. These results depend only on the smaller heat capacity of land compared to ocean and the nonlinearity of the temperature dependence of surface infra-red emission.

In section 2, we describe our idealized GCM simulations and also analyze the high latitude surface temperature change of two more comprehensive Earth system models under a high emissions scenario. In section 3, we use a simple surface energy balance model to show that the enhanced Arctic continent winter warming arises through the combination of the smaller land surface heat capacity and the nonlinearity of the temperature dependence of surface longwave emission. This can also be understood by using a forced damped oscillator model. In section 4, we discuss the seasonality of high latitude atmospheric temperature change, which is surface-enhanced in winter as the atmosphere is near radiative-advective equilibrium, but more vertically homogeneous in summer as the Arctic land gets warm enough to trigger convection. In section 5, we conclude and discuss the implications and limitations of this study.

2. Experiments with General Circulation Models

We use the Isca climate modeling framework (Vallis et al. 2018) in a fairly spare configuration. Specifically, we have no clouds or sea ice, and a slab ocean boundary condition, with a simple representation of land following present-day continental outlines. We impose a seasonal cycle of insolation and use the comprehensive SOCRATES radiation scheme for both solar and infra-red radiation (Manners et al. 2017; Thomson and Vallis 2019), with a constant surface albedo equal to 0.3 everywhere. In the form used here SOCRATES maintains good accuracy with CO_2 levels up to a factor of 16 more than today. Land differs from oceans only by the depth of its mixed layer and hence its surface heat capacity, which we set to 2 meters equivalent water depth for continents and 20 meters for oceans, and by the roughness constant, which is set to be 10 times higher over land than ocean. We use today's distribution of continents. (The continents in the Eocene were different from today's but not appreciably so and land masses such as North America, Greenland, and Europe are still recognizable.) Simulations are run at spectral T42 resolution, which corresponds to approximately 2.8 degrees resolution at the equator. Convection is calculated using a simplified Betts-Miller convection scheme (Frierson 2007). Large scale condensation is parametrized such that relative humidity does not exceed one, and condensed water immediately returns to the surface. This configuration thus (deliberately) excludes cloud feedbacks and effects of land-surface changes, but maintains land-ocean contrasts and potential radiative-convective effects.

We first describe three simulations in which CO_2 concentrations are set to 300 ppm, 1200 ppm ($4\times$300ppm), and 4800 ppm ($4\times$1200ppm) respectively. Given the logarithmic nature of CO_2 forcing with respect to concentration, the additional greenhouse effect from each quadrupling is similar, being just slightly higher for the second quadrupling than for the first (not shown). Later, we discuss 'all-land' and 'all-ocean' experiments, in which the depth of the mixed layer is set to 2 m and 20 m respectively over the whole surface.

The total atmospheric heat transport is remarkably constant across the three experiments, with the increase in moist atmospheric heat transport (arising from the higher temperature)

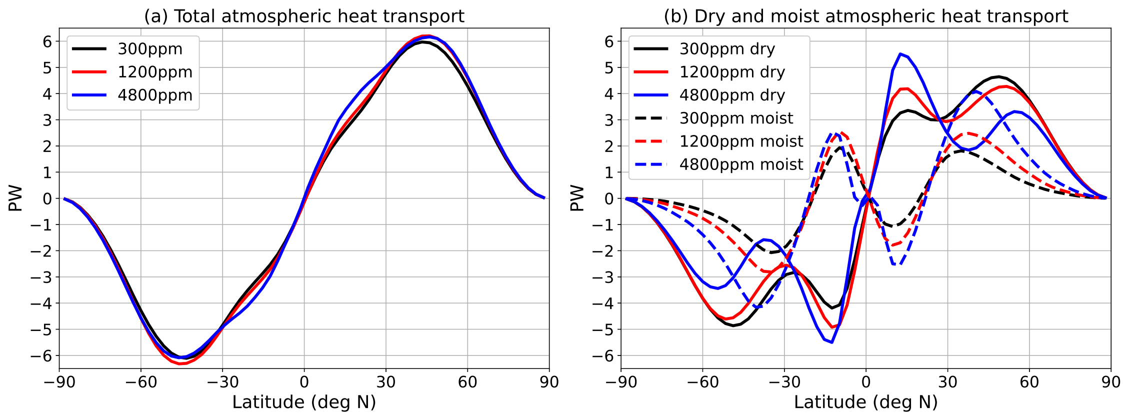

FIG. 1. Atmospheric heat transport. Total (a), dry and moist (b) northward atmospheric heat transport for the 300 ppm (black), 1200 ppm (red), 4800 ppm (blue) simulations.

being almost perfectly compensated by a decrease in dry atmospheric heat transport (fig. 1). Consequently, the mid-tropospheric temperature gradient is about the same in all experiments. However, the surface meridional temperature gradient falls considerably with increased CO_2 levels with increased high-latitude temperatures, enhanced over land in winter. The annual-mean surface temperature for land (solid) and ocean (dashed) for the control simulation (black) and increased CO_2 simulations is shown in Figure 2a. Panel (b) shows the surface temperature change as CO_2 is increased from 300 ppm to 1200 ppm and from 1200 ppm to 4800 ppm. Despite the absence of sea ice, the surface temperature change is polar amplified as the high latitude atmosphere warms more near the surface in the absence of convection (Henry et al. 2020). The surface temperature change is about twice as large for the second quadrupling (1200 ppm to 4800 ppm) than for the first (300 ppm to 1200 ppm). This is mostly due to the much larger increase in absorbed solar energy for the second quadrupling as the atmosphere is warmer and moister (fig. 3), the top-of-atmosphere forcing is also slightly larger in the extratropics for the second quadrupling (not shown). In this set of simulations the land and ocean warm by similar amounts in the tropics and midlatitudes, stemming from the fact that the evaporation is similar over the land as over the ocean and the air above land is as moist as the air above ocean (Byrne and O'Gorman 2013). If the land evaporative resistance is reduced the land does warm more than the ocean (not shown).

Figure 2c shows the surface temperature averaged poleward of 70 degrees North for land (solid) and ocean (dashed) for the control (black) and increased CO_2 simulations (1200 ppm in blue and 4800 ppm in red). The land temperatures stay above 273 K almost

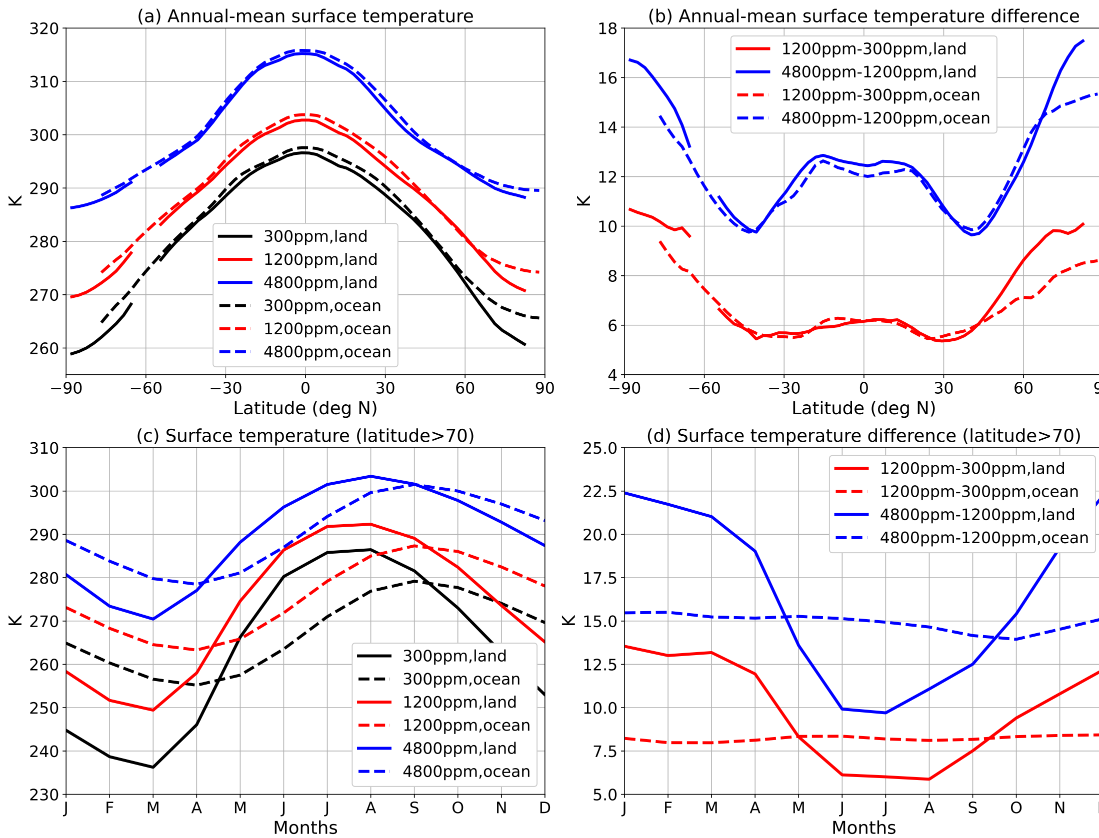

FIG. 2. (a) Surface temperature over land (solid) and ocean (dashed) for the 300 ppm (black), 1200 ppm (blue), 4800 ppm (red). (b) Surface temperature change over land and ocean between the 300 ppm and 1200 ppm simulations (blue) and the 1200 ppm and 4800 ppm simulations (red). (c) Seasonality of surface temperature North of 70 degrees latitude for land (solid) and ocean (dashed) for the 300 ppm (black), 1200 ppm (blue), and 4800 ppm (red) experiments. (d) Surface temperature change North of 70 degrees latitude for land (solid) and ocean (dashed) between the 300 ppm and 1200 ppm simulations (blue) and the 1200 ppm and 4800 ppm simulations (red).

year-round in the 4800 ppm simulation. Figure 2d shows the difference between the 300 ppm and 1200 ppm simulations (blue) and the 1200 ppm and 4800 ppm simulations (red). There is a clear seasonality in land surface temperature change: for the difference between 300 ppm and 1200 ppm, it reaches 13 degrees in winter and 6 degrees in summer, whereas ocean surface temperature change is around 8 degrees year-round.

Figure 4 shows the atmospheric temperature change between the 300 ppm and 1200 ppm simulations (a,b) and between the 1200 ppm and 4800 ppm simulations (c,d) for winter

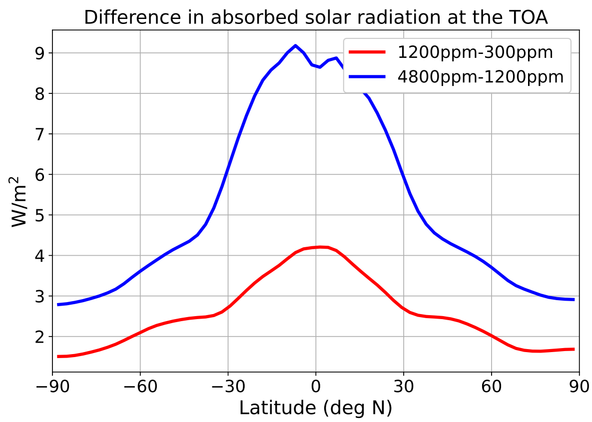

FIG. 3. Change in absorbed solar radiation at the top-of-atmosphere between the 300 ppm and 1200 ppm simulations (blue) and the 1200 ppm and 4800 ppm simulations (red).

(a,c) and summer (b,d). For the first quadrupling (a,b), the high latitude temperature change is surface-enhanced in winter and top-heavy in summer. For the second quadrupling (c,d), the high latitude temperature change is top-heavy year-round, but more so in summer. The seasonality of atmospheric temperature change is investigated in section 4.

Comprehensive climate model simulations of a high anthropogenic emissions scenario also show enhanced warming over high latitude land in winter, even when Arctic sea ice has melted. Figure 5 shows results from two comprehensive climate models: the Canadian Earth System Model 5 (CanESM5) and the coupled model 6 from the Institut Pierre Simon Laplace (IPSL-CM6A-LR) under a high emissions scenario (the Shared Socioeconomic Pathway 5-8.5 (SSP5-8.5)). Panels a and c show the monthly Northern hemisphere sea ice area. Panels b and d show the Arctic land (solid) and Arctic ocean (dashed) surface temperature change between 2270-2300 and 2150-2180. For both models, once the sea ice is melted the Arctic land warms more in winter and less in summer than does the Arctic ocean, which warms uniformly throughout the year. We note that the two averaging periods (2270-2300 and 2150-2180) do not correspond to a climate in equilibrium, unlike the idealized model simulations. Differences in cloud feedbacks, ocean circulation and other processes may explain why the two models differ quantitatively. However, their results are generally consistent with each other and with the results of our more idealized model. This prompts us to seek a simpler, robust explanation of the seasonality of high latitude warming.

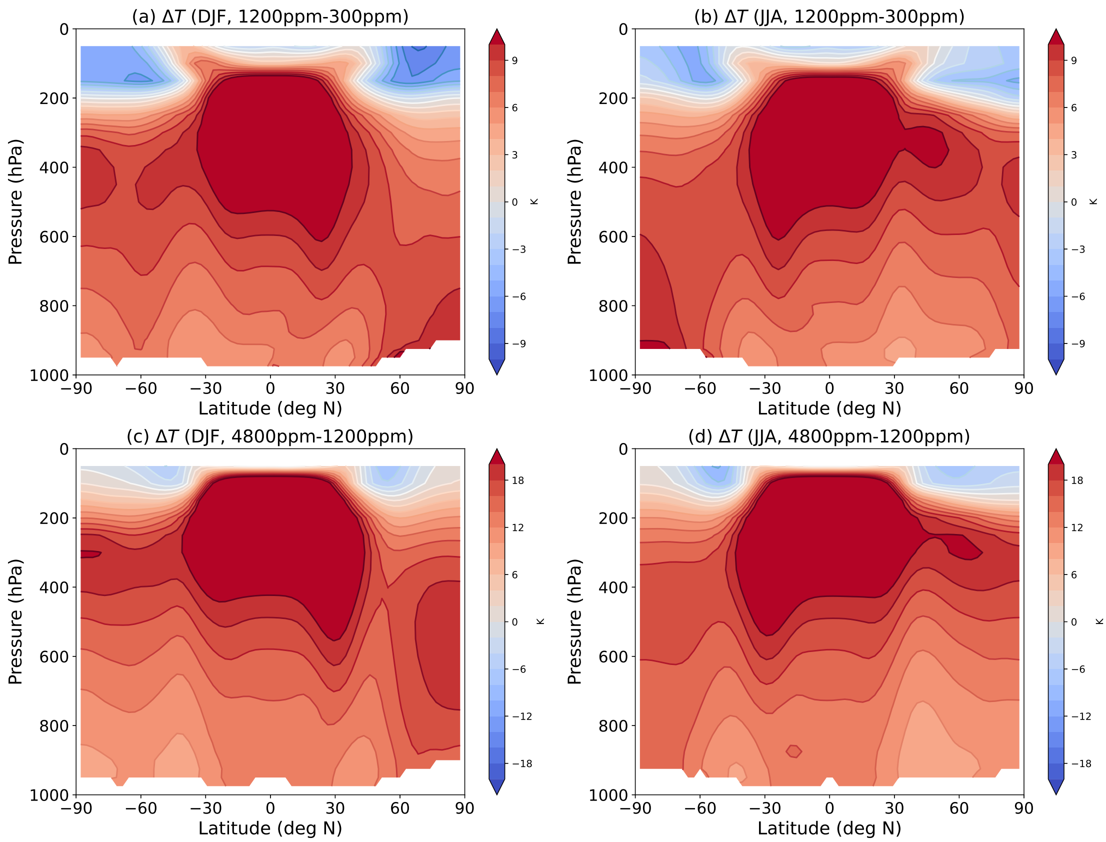

FIG. 4. Atmospheric temperature change between the 300 ppm and 1200 ppm simulations (a,b) and between the 1200 ppm and 4800 ppm simulations (c,d) for Northern Hemisphere winter (a,c) and summer (b,d).

3. Seasonality of surface temperature change

We use a simple surface energy balance model to better understand the seasonality of high latitude surface temperature. The surface energy balance in the model is given by

$$C\frac{\mathrm{d}T_S}{\mathrm{d}t} = \mathrm{SW_{net}} + \mathrm{LW_{down}} - \sigma T_S^4 + \mathrm{SH} + \mathrm{LH}, \quad (1)$$

where C is the surface heat capacity (equal to $8.3 * 10^7 J/m^2/K$ for the ocean surface and $8.3 * 10^6 J/m^2/K$ for the land surface), T_S is the surface temperature, t is time, $\mathrm{SW_{net}}$ is the net downwelling shortwave radiative flux at the surface, $\mathrm{LW_{down}}$ is the downwelling longwave radiative flux at the surface, σ is the Stefan-Boltzmann constant (so that σT_S^4 is the upwelling longwave radiative flux emitted from the surface), SH is the sensible heat

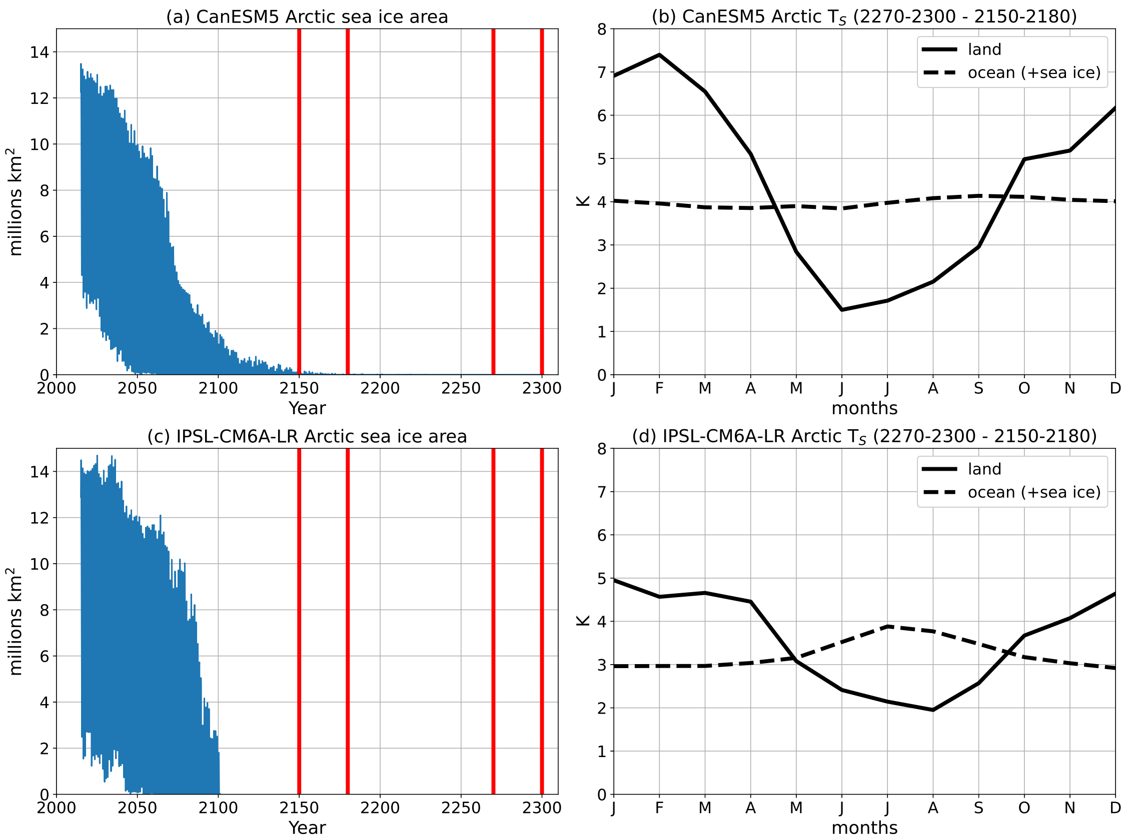

FIG. 5. Seasonality of Arctic land and ocean surface temperature change in two comprehensive climate models in a high emissions scenario when Northern hemisphere sea ice almost vanishes. Monthly Arctic sea ice area (blue shading) with the averaging limits in red (2150, 2180, 2270, 2300) (a,c). Arctic land (solid) and ocean (dashed) surface temperature change between 2270-2300 and 2150-2180 (b,d). The emissions scenario is the Shared Socioeconomic Pathway 5-8.5 (SSP5-8.5). The two models used are the Canadian Earth System Model 5 (CanESM5) (a,b) and the coupled model 6 from the Institut Pierre Simon Laplace (IPSL-CM6A-LR) (c,d). Those were the only models available which extended to 2300 in the SSP5-8.5 scenario. Arctic surface temperatures are averaged poleward of 70 degrees North. Note that the data for sea ice area for IPSL-CM6A-LR stops at year 2100.

flux and LH the latent heat flux from the atmosphere to the surface. The quantities T_S $\mathrm{SW_{net}}$, $\mathrm{LW_{down}}$, SH, and LH are functions of time but not space. We use values from the GCM integrations for C, $\mathrm{SW_{net}}$, $\mathrm{LW_{down}}$, SH, and LH, averaged poleward of 70 degrees North, such that the only free variable is T_S, and for any given parameter set we integrate over 10 years, or until the model is in a seasonally-varying steady state.

Figure 6 shows the input to the surface energy balance model, focusing on the difference between the 300 ppm and 1200 ppm simulations. Panel (a) shows the net shortwave radiation at the surface for the 300 ppm (black) and 1200 ppm (blue) simulations. The increased atmospheric absorption of solar radiation leads to a small decrease in shortwave flux at the surface. Panel (b) shows the downwelling longwave radiation at the surface for land (solid) and ocean (dashed). The increase in downwelling longwave is approximately the same over ocean and land and has a seasonal cycle, which could also contribute to the seasonality in surface warming. Panel (c) shows the seasonal cycle of evaporative cooling over land and ocean. While it is small year-round over ocean and in winter over land, it is comparable to downwelling longwave radiation in summer over land. Moreover, there is an increase in evaporative cooling over land during the summer and over ocean during the winter. This pattern could also contribute to differences in seasonality of warming over land and ocean.

Figure 7a shows results from the surface energy balance model, comparing the seasonality of surface temperature change over land and ocean with results from the GCM data for the difference between the 300 ppm and 1200 ppm simulations. The simple model fits the GCM data quite well, which is expected since all the terms of equation (1) except the surface temperature evolution itself are taken from the GCM. We can now use the simple model to explore the main drivers of the difference in surface temperature change between high latitude ocean and land.

To isolate the causes of the seasonality, we remove the surface fluxes (SH and LH) and the seasonality of the change in downwelling longwave radiation at the surface from equation (1); that is, the change in downwelling longwave radiation is replaced by its average change over time (45 W/m^2). Figure 7b compares the surface energy balance model with the GCM data in the same way as Figure 7a. Without the evaporative cooling over land in summer, the surface temperature in the simple surface energy balance model gets significantly warmer over land in summer for both the 300ppm and 1200ppm simulations (not shown), but this does not affect the surface temperature change. The increase in evaporative cooling over ocean in winter leads this simple model to overestimate the warming year-round as seasonal differences in fluxes are smoothed out in time by the ocean's large surface heat capacity. The change in evaporative cooling and downwelling longwave radiation seemed like good candidate explanations for the difference in seasonality of warming over land and ocean. However, the land surface temperature in the simple surface energy balance model still has a large seasonality compared to that of the ocean.

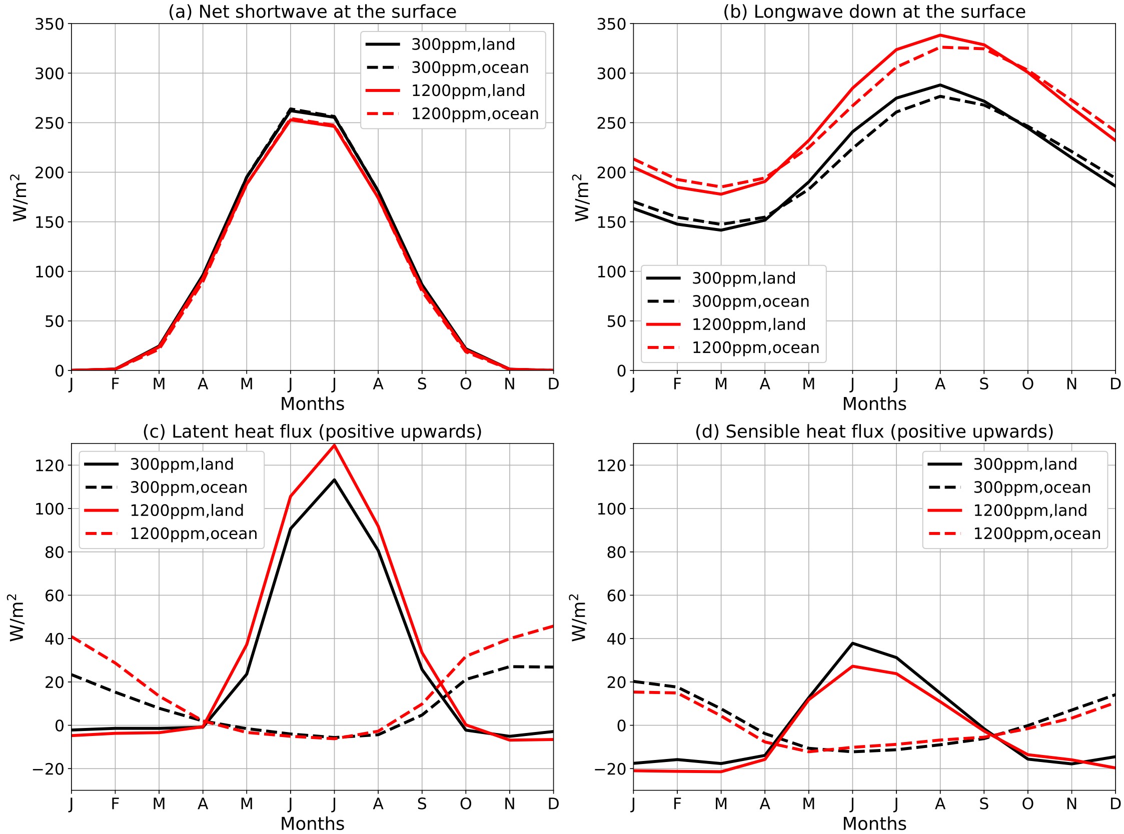

FIG. 6. Inputs to the surface energy balance model prescribed from the GCM. Values for the 300 ppm (black) and 1200 ppm (blue) over land (solid) and ocean (dashed) are averaged poleward of 70 degrees North. (a) Net shortwave radiation at the surface (positive downwards). (b) Downward longwave radiation at the surface (positive downwards). (c) Evaporative cooling at the surface (positive upwards). (d) Sensible heat flux at the surface (positive upwards).

The two aspects of the simple surface energy balance model that yield the difference in seasonality in surface temperature change between land and ocean are the surface heat capacity (C) and the nonlinearity of the temperature dependence of the surface longwave emission (σT_S^4). A smaller heat capacity implies that less energy is required to change the temperature of the surface, hence the climatological seasonality of land is larger and any energy perturbation to the surface has a more immediate impact on surface temperature. Furthermore, the nonlinearity of σT_S^4 means that, for a smaller starting temperature, a larger increase in temperature is required to reach a given increase in longwave emission and balance the new forcing.

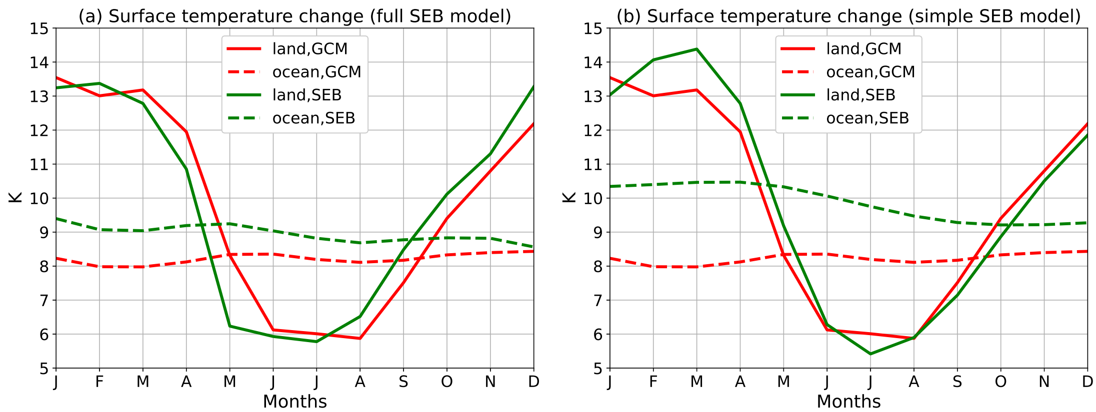

FIG. 7. Surface energy balance model results. (a) The full surface energy balance model (green) accurately reproduces the GCM data (red). (b) The simple surface energy balance model (green), with no surface fluxes and no seasonality in the change in downwelling longwave radiation at the surface, reproduces the patterns of land (solid) and ocean (dashed) surface temperature change.

The higher climatological seasonality of land surface temperatures means that the land's temperature response will also have a large seasonality: the temperature response will be larger when the starting temperature is low (in winter) and smaller when the starting temperature is high (in summer). The ocean's large surface heat capacity means the climatological seasonality is smaller (25 K versus 50 K for land), and that any energy perturbation's impact on surface temperature will be smoothed out and affect the annual mean temperature change, rather than a given month.

The above results can be straightforwardly interpreted as a damped forced oscillator obeying the equation

$$C\frac{\mathrm{d}T}{\mathrm{d}t} = -\sigma T^4 + A\cos\omega t + D, \tag{2}$$

where A is the amplitude of the seasonal forcing and D is a constant representing the time-invariant components of the forcing. If the seasonal cycle is not too large we can linearize temperature around some mean temperature $\overline{T}$ to give

$$C\frac{\mathrm{d}T'}{\mathrm{d}t} = -MT' + A\cos\omega t, \tag{3}$$

	Ocean, 260K	Land, 280K	Ocean, 280K	Land, 260K
C ($10^6\,\mathrm{J\,m^{-2}K^{-1}}$)	83	8.3	83	8.3
M ($\mathrm{W\,m^{-2}K^{-1}}$)	4.98	4.98	3.99	3.99
T_0 (K)	14.7	58.1	14.5	48.1

TABLE 1. Amplitude of seasonal oscillation (T_0) for ocean and land surfaces and for $\overline{T} = 260\,\mathrm{K}$ and $\overline{T} = 280\,\mathrm{K}$.

where $M = 4\sigma\overline{T}^3$ and $T' = T - \overline{T} - D/M$, and we henceforth drop the prime on T. The solution of (3), after transients have died, is $T = T_0 \cos(\omega t + \phi)$ where

$$T_0 = \frac{A}{\left(C^2\omega^2 + M^2\right)^{1/2}} \quad \text{and} \quad \phi = \frac{C\omega}{M}. \tag{4}$$

The amplitude of the seasonal oscillation (i.e. T_0) naturally diminishes for larger C, so that the seasonal cycle over land is larger than that over the ocean. Less obviously, the amplitude diminishes as K increases, and since K is a function of temperature, a warmer climate will have a smaller seasonal cycle (at least to the extent that the seasonal cycle is described by (1) and (2)).

Putting in a few numbers, for 2 m of water at 270 K we find $C\omega \approx 1.6\,\mathrm{W/(m^2\,K)}$ and $M = 4.5$ W/(m^2 K), so the heat capacity and temperature effects are evidently comparable and changes in both may be important. Table 1 shows values of the amplitude of the seasonal oscillation for the high latitude land and ocean for $T_0 = 260\,\mathrm{K}$ and $T_0 = 280\,\mathrm{K}$. The amplitude of the seasonal oscillation (T_0) is almost the same for the two values for the ocean, whereas it is reduced by 10K for land, generally consistent with our simulation results (fig. 2).

4. Seasonality of atmospheric temperature change

Changes in downwelling longwave radiation at the surface are coupled to the surface temperature change and they should not be considered as independent variables. Nevertheless, in these simulations, the downwelling longwave radiation at the surface does not differ much between land and ocean while the surface temperatures do (fig. 2c and fig. 6b). This can also be seen in the atmospheric temperatures over land and ocean:

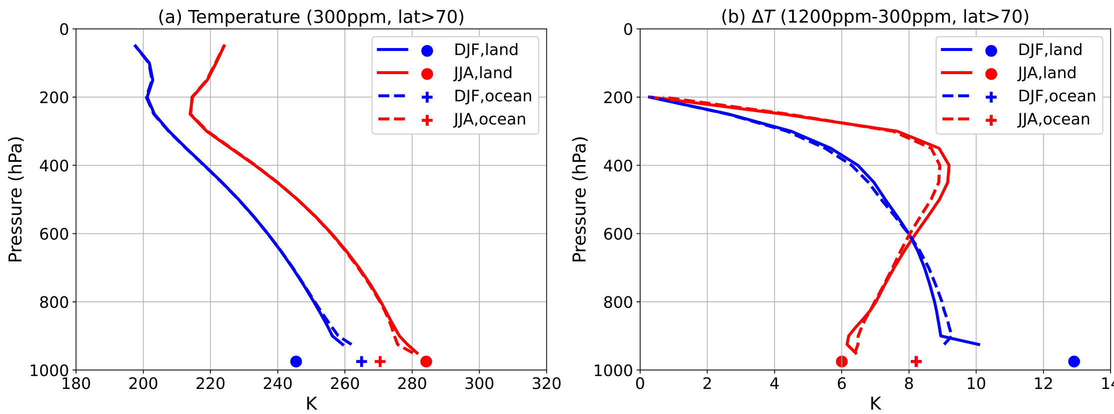

FIG. 8. (a) Atmospheric and surface temperature over ocean (dashed, cross) and land (solid, dot) for winter (blue) and summer (red) poleward of 70 degrees North. (b) Atmospheric and surface temperature change between the 300 ppm and 1200 ppm simulations. Note that the ocean surface temperature change points overlap.

fig. 8a shows the atmospheric and surface temperature averaged poleward of 70 degrees North over ocean (dashed, cross) and land (solid, dot) for the winter (blue) and summer (red) months. Figure 8b shows the atmospheric and surface temperature change between 300 and 1200 ppm simulations. While the ocean's climatological surface temperature and surface temperature change have a small seasonality compared to land, the atmospheric temperature and atmospheric temperature change are the same. This suggests that while surface temperatures over land and ocean can remain relatively uncoupled, atmospheric temperatures tend to homogenize.

Figure 9 shows the convective, advective, and radiative temperature tendencies over land and ocean for the 300 ppm simulation poleward of 70 degrees North, for Northern Hemisphere winter and summer. In winter, advection warms the atmosphere near the land surface and cools the atmosphere near the ocean surface, and vice-versa in summer. That is, advection acts to homogenize the near-surface atmospheric temperatures over land and ocean. We also see that the main equilibrium is between radiation and advection, except over land during summer when convection is triggered and the main equilibrium is between radiation and convection. This explains the surface enhanced warming in winter and more vertically homogeneous warming in summer (Figure 4). Finally, there is convection over ocean in winter which may be due to the ocean surface being warmer than the atmosphere in winter because of its high heat capacity.

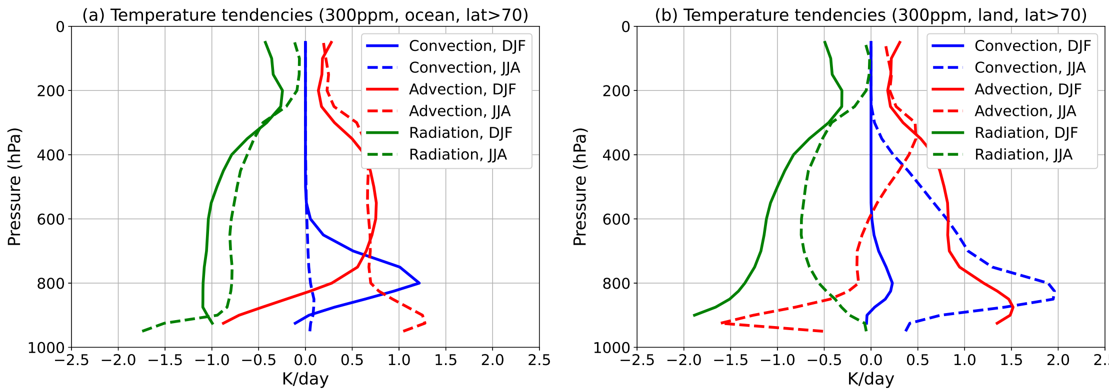

FIG. 9. Atmospheric temperature tendency budget for the 300 ppm simulation over ocean (a) and land (b) for latitudes poleward of 70 degrees North. It shows the convective (blue), advective (red), and radiative (green) temperature tendencies for Northern hemisphere winter (solid) and summer (dashed).

To clarify the relationship between the atmospheric energy balance and vertical temperature change structure, we run "all-land" and "all-ocean" simulations where the aquaplanet's mixed layer depth is uniformly 2m and 20m respectively at 300 ppm and 1200 ppm. Figure 10 is analogous to fig. 8 but for the "all-ocean" and the "all-land" experiments. The higher surface heat capacity in the "all-ocean" experiments results in a very small seasonal cycle in surface and atmospheric temperature, and temperature change. Inversely, the seasonal cycle is very large for the "all-land" experiment (approximately 55K for the surface temperature), and the surface temperature change is higher in winter (13.5K) and lower in summer (5.8K). The vertical structure of atmospheric temperature change is moreless homogeneous in the "all-ocean" experiment. However, in the "all-land" experiment, warming is bottom-heavy in winter and top-heavy in summer. Figure 11 is analogous to fig. 9 but for the "all-ocean" and the "all-land" experiments. In the "all-land" experiments, there is a clear seasonality between radiative-convective equilibrium in summer and radiative-advective equilibrium in winter. In the "all-ocean" experiments, the atmosphere is close to radiative-advective equilibrium year-round, with slightly more advection in winter.

These two additional simulations show that the atmospheric temperature change in the initial simulations is a mix of these two extremes ("all-land" and "all-ocean"), with advection smoothing out the differences in atmospheric temperature driven by the differing surface temperatures of ocean and land. The vertical structure of high latitude temperature change is driven by what happens at the surface: if it gets warm enough at the

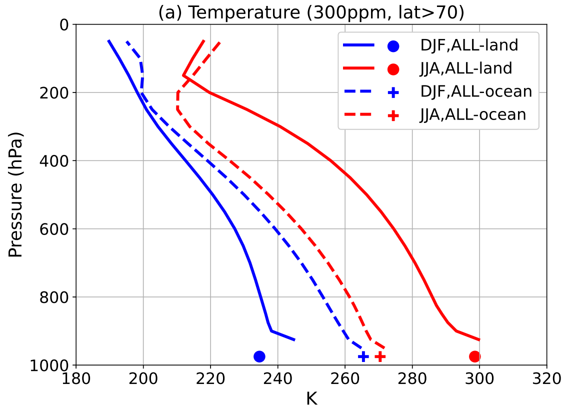

FIG. 10. Same as Figure 8 but for "all-ocean" and "all-land" simulations, which are two separate sets of simulations where the mixed layer depth is set uniformly to 20m and 2m respectively.

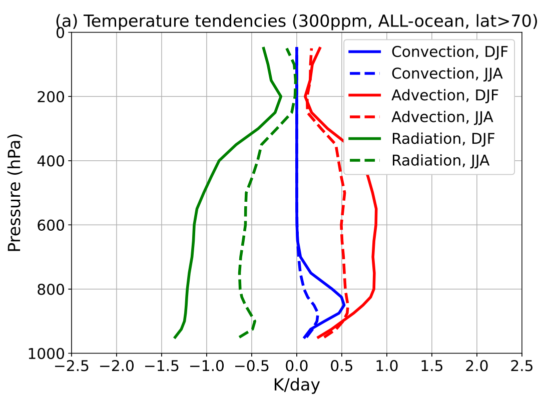

FIG. 11. Same as Figure 9 but for "all-ocean" and "all-land" simulations, which are two separate sets of simulations where the mixed layer depth is set uniformly to 20m and 2m respectively.

surface, deep convection is triggered, which causes vertical mixing and a more vertically homogeneous atmospheric warming. In the absence of convection, the main balance is between advective warming and radiative cooling and atmospheric warming is enhanced near the surface (Cronin and Jansen 2016, Henry et al. 2020). Since the high latitude land gets warm enough in summer to trigger deep convection, the warming is more vertically homogeneous. For the difference between the 1200 ppm and 4800 ppm simulations, there is deep convection triggered year-round at high latitudes, hence the atmospheric warming is never enhanced near the surface (fig. 4).

5. Discussion and Conclusions

Various lines of evidence suggest that, as greenhouse gases increase, the Arctic land warms more in winter and less in summer, thus reducing the seasonality over land in warm climates. In this paper we have identified a robust mechanism for this that applies both to the warm climates of the past and to the expected warming of the future. The reduced seasonality may contribute to the reason that the some of the warm climates of the past were able to sustain above freezing year-round temperatures, even in continental winters at high latitudes and without excessively warm tropical temperatures. The early Eocene, for example, had a reduced surface latitudinal surface temperature gradient and its Arctic continents had especially warm winters compared to those of today. Similarly, current warming trends and projections of future warming show a polar amplified surface temperature change and more Arctic warming in winter.

Experiments with an idealized GCM show that the surface temperature change from increasing CO_2 is polar amplified, even in the absence of sea-ice effects. This is, however, only a near-surface phenomenon — the meridional temperature gradient in mid-atmosphere and the total meridional atmospheric heat transport are virtually unchanged: the increase in energy transport by moist processes (because the atmosphere is warmer and wetter) is closely compensated by a decrease in dry atmospheric heat transport. The increase in Arctic land surface temperature is twice as large in winter as in summer. And, the seasonality of the vertical structure of Arctic warming is consistent with recent warming trends: surface-enhanced in winter and more vertically homogeneous in summer. Similar results are found in two comprehensive climate models under a high emissions scenario; specifically, even after all sea ice is melted, Arctic land continues to warms more in winter than summer by at least a factor of two, whereas the ocean continues to warm uniformly throughout the year.

The seasonality of high-latitude land warming can be explained with a simple surface energy balance model. The combination of the small surface heat capacity of land (which leads to a large climatological seasonality in temperature over land) and the nonlinearity of the temperature dependence of surface longwave emission (which leads to cold temperatures warming more as CO_2 increases) is largely responsible for the reduction in seasonality over land as CO_2 levels increase. The downward infra-red radiation, which is one of the primary forcings of surface temperature, is actually fairly similar over land and ocean because advection smooths out differences in near-surface atmospheric temperature over land and ocean.

An understanding of the atmospheric warming then follows by connecting the changes in the surface energy balance to the mechanisms determining the vertical structure temperature. The vertical structure of high-latitude warming differs considerably from that in tropics. In the latter the warming is top-heavy because the atmosphere is near radiative-convective equilibrium and the atmospheric temperature profile more-or-less follows a moist adiabat. In contrast, in much of the high latitudes (especially in winter) the atmosphere is near radiative-advective equilibrium and this promotes surface-enhanced atmospheric warming (Payne et al. 2015; Henry et al. 2020). In the first quadrupling of CO_2, convection is only triggered over land in summer, which leads to surface-enhanced warming in winter and more vertically homogeneous warming in summer. Consistently, in “all-ocean" simulations the Arctic atmosphere is in radiative-advective equilibrium year-round and the warming is surface-enhanced. In “all-land” simulations, there is a clear seasonality between radiative-convective summer, with top-heavy warming, and radiative-advective winter with surface-enhanced warming.

The mechanisms we have identified apply to both warm past climates and potentially warm future climates. The main differences between the two, in reality, are the continental configuration, the vegetation, and the presence of sea and land ice and these will, of course, have quantitative effects. We have also neglected the presence of clouds, and he fact that convection does occur over high-latitude land in winter suggests that cloud feedbacks may be increasingly important in warm climates (e.g., Abbot and Tziperman 2008; Cronin and Tziperman 2015). Similarly, the continuing reduction of sea ice is likely to affect the seasonality of Arctic warming in climates of the near future. A quantitative picture of the seasonality at high-latitudes, and how it may differ in warm climates, will require full consideration of the interaction of lapse rate changes, sea ice, surface heat storage, ocean circulation effects, clouds and potentially other factors. The path toward that picture will require an understanding of the role of these various components in isolation as well as acting as a whole.

Acknowledgments. We wish to thank all the Isca team for many discussions about climate and modeling, and especially Stephen Thomson and Ruth Geen for help with the model setup and analysis. We also thank Eli Tziperman and Camille Hankel for a number of fruitful conversations about polar climates. This work was supported by NERC under a NERC-NSF partnership.

Data availability statement: The code to reproduce the figures is available at https://github.com/matthewjhenry/simple-seasonality-arctic and the data is available at https://zenodo.org/record/4529135.

References

Abbot, D. S., and E. Tziperman, 2008: Sea ice, high-latitude convection, and equable climates. *Geophysical Research Letters*, **35 (3)**.

Beerling, D. J., and D. L. Royer, 2011: Convergent cenozoic CO_2 history. *Nature Geoscience*, **4 (7)**, 418–420.

Bintanja, R., and E. Van der Linden, 2013: The changing seasonal climate in the arctic. *Scientific reports*, **3 (1)**, 1–8.

Byrne, M. P., and P. A. O'Gorman, 2013: Land-ocean warming contrast over a wide range of climates: Convective quasi-equilibrium theory and idealized simulations. *J. Climate*, **26**, 4000–4016.

Cronin, T. W., and E. Tziperman, 2015: Low clouds suppress arctic air formation and amplify high-latitude continental winter warming. *Proceedings of the National Academy of Sciences*, **112 (37)**, 11 490–11 495.

Eberle, J. J., H. C. Fricke, J. D. Humphrey, L. Hackett, M. G. Newbrey, and J. H. Hutchison, 2010: Seasonal variability in arctic temperatures during early eocene time. *Earth and Planetary Science Letters*, **296 (3-4)**, 481–486.

Evans, D., and Coauthors, 2018: Eocene greenhouse climate revealed by coupled clumped isotope-Mg/Ca thermometry. *Proc. Nat. Acad. Sci.*, **115 (6)**, 1174–1179.

Frierson, D. M., 2007: The dynamics of idealized convection schemes and their effect on the zonally averaged tropical circulation. *J. Atmos. Sci.*, **64 (6)**, 1959–1976.

Henry, M., T. M. Merlis, N. J. Lutsko, and B. E. J. Rose, 2020: Decomposing the drivers of polar amplification with a1single column model. *Journal of Climate*, **submitted**, doi:10.31223/osf.io/dzmvq, URL https://eartharxiv.org/dzmvq.

Holland, M. M., and C. M. Bitz, 2003: Polar amplification of climate change in coupled models. *Climate Dyn.*, **21 (3-4)**, 221–232.

Huber, M., and R. Caballero, 2011: The early eocene equable climate problem revisited. *Climate of the Past*.

Hwang, Y.-T., and D. M. Frierson, 2010: Increasing atmospheric poleward energy transport with global warming. *Geophysical Research Letters*, **37 (24)**.

Hwang, Y.-T., D. M. W. Frierson, and J. E. Kay, 2011: Coupling between Arctic feedbacks and changes in poleward energy transport. *Geophys. Res. Lett.*, **38**, L17 704.

Lu, J., and M. Cai, 2009: Seasonality of polar surface warming amplification in climate simulations. *Geophysical Research Letters*, **36 (16)**.

Lunt, D. J., and Coauthors, 2012: A model–data comparison for a multi-model ensemble of early eocene atmosphere–ocean simulations: Eomip. *Climate of the Past*, **8**, 1717–1736.

Manners, J., J. M. Edwards, P. Hill, and J.-C. Thelen, 2017: SOCRATES: Suite Of Community RAdiative Transfer codes based on Edwards and Slingo. Tech. rep., UK Met Office, 87 pp.

Payne, A. E., M. F. Jansen, and T. W. Cronin, 2015: Conceptual model analysis of the influence of temperature feedbacks on polar amplification. *Geophys. Res. Lett.*, 9561–9570.

Pearson, P. N., B. E. van Dongen, C. J. Nicholas, R. D. Pancost, S. Schouten, J. M. Singano, and B. S. Wade, 2007: Stable warm tropical climate through the eocene epoch. *Geology*, **35 (3)**, 211–214.

Pithan, F., and T. Mauritsen, 2014: Arctic amplification dominated by temperature feedbacks in contemporary climate models. *Nat. Geosci.*, **7**, 181–184.

Taylor, P. C., M. Cai, A. Hu, J. Meehl, W. Washington, and G. J. Zhang, 2013: A decomposition of feedback contributions to polar warming amplification. *J. Climate*, **26**, 7023–7043.

Thomson, S. I., and G. K. Vallis, 2019: The effects of gravity on the climate and circulation of a terrestrial planet. *Quarterly Journal of the Royal Meteorological Society*, **145 (723)**, 2627–2640.

Vallis, G. K., and Coauthors, 2018: Isca, v1. 0: A framework for the global modelling of the atmospheres of earth and other planets at varying levels of complexity.

Winton, M., 2006: Amplified Arctic climate change: What does surface albedo feedback have to do with it? *Geophys. Res. Lett.*, **33**, L03 701.